

Optical tight-binding model of computer-generated holograms in vector representation

I-Lin Ho^{1, a)}

*ChiMei Visual Technology Corporation, Tainan 741, Taiwan,
R.O.C.*

(Dated: 25 July 2019)

This research presents an efficient vector diffraction theory to calculate transmissive fields of computer-generated holograms (CGH) with pixels at a subwavelength scale. On the basis of the tight-binding presumption, we consider the transmissive fields on the exit surface to tightly bind with the pixels to which they belong, and to have limited couplings with fields of surrounding pixels. In this way the transmissive field of an individual pixel can be efficiently determined by a transfer matrix with finite basis sets that state the conditions of nearby pixels, called the optical tight-binding model (OTB). Accurate optics via the finite difference time domain (FDTD) calculations show that the predicted intensity by OTB agree with a fractional error from the target one. The results conclude that this proposed algorithm outperforms the most frequently used alternatives by one or two orders of magnitude in accuracy for thin holograms and an acceptable computational cost.

^{a)}Electronic mail: sunta.ho@msa.hinet.net

The intensity profile of optical fields can be manipulated by using a computer-generated digital phase raster, also called a computer-generated hologram (CGH). Physically, CGH is illuminated by a monochromatic beam that is relayed to a focusing objective, and the intensity distribution is produced at the focal plane of the objective. The hologram in general is implemented in a spatial light modulator (SLM)^{1,2} or similar technology, and leads to a wide range of applications utilizing CGHs³⁻⁶. In recent decades, with great progress on photo-lithography technology, fabricating optical elements with pixel pitch at the subwavelength scale has become feasible and economical⁷. The emerging vectorial effect of a light beam accordingly encourages more advanced applications, such as the vector holographic optical trap and metalens⁸⁻¹⁰, but brings forth the issue about the invalidation⁸ of the conventional scalar diffraction theory (SDT)^{11,12}.

In contrast to SDT, calculating CGH by rigorous electromagnetic computational methods to generate a high-quality arbitrary intensity distribution is still a challenging problem, due to the costly computation resources associated with its area, the lack of periodicity, the excessive pixel parameters, and the interactive vector states of pixel fields obeying Maxwell's equations. Up to now, a small amount of literature has reported on designing CGHs with a sub-wavelength pixel size, including the micro-genetic algorithm FDTD method¹³ using time-consuming searching characters, the Gerchberg-Saxton-algorithm FDTD method¹⁴ that is valid for particular paraxial functions, the iterative optimization algorithm¹⁵ for aperiodic 1D beam splitters, and the two-step genetic algorithm⁸ for 2D μm -scale beam splitters. In this paper, we describe an efficient vector diffraction theory, the optical tight-binding (OTB) model, to design macroscopic (mm- to cm-scale diameter) CGHs functioning under arbitrary intensity profiles.

Before giving the mathematical details of the OTB model, we briefly discuss common operations on CGH problems: design a CGH that will convert a light field $\vec{E}_{ij,\text{in}}$ at the input plane of CGH into a target intensity distribution $I_{pq,\text{targ}}$ at the focal plane of the focusing optics (see Fig. 1). Here, the suffixes (i,j) and (p,q) index the pixel coordinates at the input plane of CGH and at the focal plane, respectively. This work adopts the simulated annealing (SA) optimization operations¹² to enable the treatment of vector states of light. The SA operations can be decomposed into several steps as in Fig. 1. In the initialization step, a guess CGH pattern, as well as the mathematically corresponding optical transfer matrix $\mathbf{T}_{ij}^{(0)}$, is given as a starting point, and the transmissive CGH fields for the first

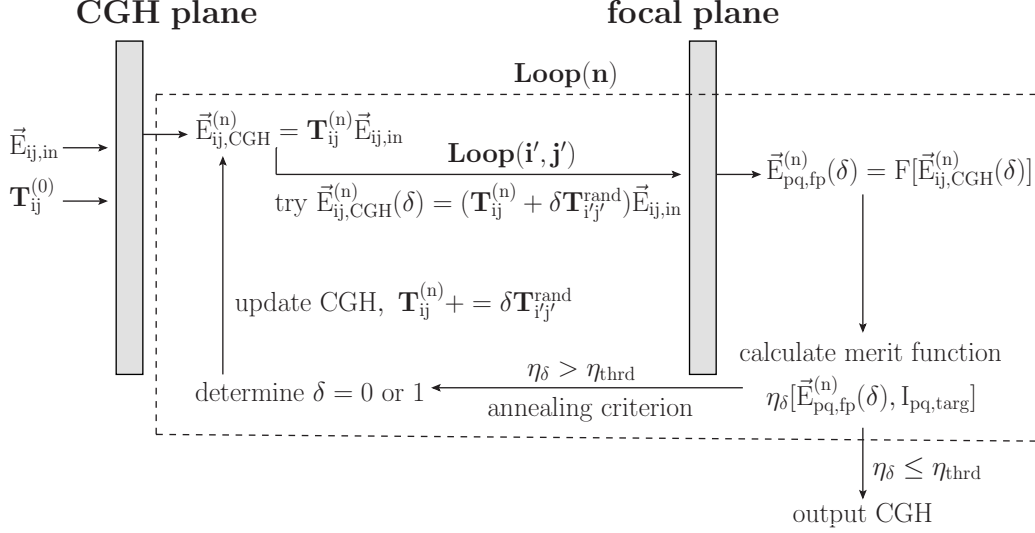


FIG. 1. Schematic of optimization on CGH problems

iteration are produced by $\vec{E}_{ij,\text{CGH}}^{(0)} = \mathbf{T}_{ij}^{(0)} \vec{E}_{ij,\text{in}}$. The temperature function $K_n = K_0/(1+n)$ of the simulated annealing specifies the range of perturbation probability during iteration n . Each iteration n of the loop begins by sequentially disturbing every CGH pixel (i', j') according to Boltzmann probability $p(\Delta\eta) = \exp(-\Delta\eta/K_n)$ with $\Delta\eta = \eta_1 - \eta_0$ (the suffixes $i'j'$ of η are omitted for simplification) to realize $I_{\text{pq,targ}}$. Here, η_δ is the figure-of-error¹² that defines the mean-square error between the reconstructed intensity $|\vec{E}_{\text{pq,fp}}^{(n)}(\delta)|^2$ and the target intensity $I_{\text{pq,targ}}$. $\eta_{\delta=1}$ and $\eta_{\delta=0}$ represent the CGH pattern after and before disturbing the pixel (i', j') , i.e. with and without a disturbed transfer matrix term $\delta \mathbf{T}_{i'j'}^{\text{rand}}$, respectively. The propagating field $\vec{E}_{\text{pq,fp}}^{(n)}(\delta) = F[\vec{E}_{ij,\text{CGH}}^{(n)}(\delta)]$ at the focal plane is modeled using a Fourier transform F , which assumes paraxial approximation for the focusing optics. The iterative loop n is terminated once the figure-of-error converges on a value below a given threshold, i.e. $\eta \leq \eta_{\text{thrd}}$.

On the basis of ray optics, conventional scalar models^{11,12,16} simplify the transfer matrix as a scalar complex coefficient $T_{ij} = \exp(i2\pi n_k d_{ij}/\lambda)$, ignoring the polarization and the amplitude attenuation. Here n_k is the refractive index of the local material, d_{ij} is the thickness of pixel ij , and λ is the light wavelength in vacuum. Figure 2 quantitatively demonstrate the validity of this scalar treatment by analyzing ensembles of 3000 binary kinoforms¹² versus pixel size Λ , using the rigorous electromagnetic computational method (rigorous coupled wave algorithm, RCWA^{17,18}, in this work). The binary kinoforms are composed of 21x21

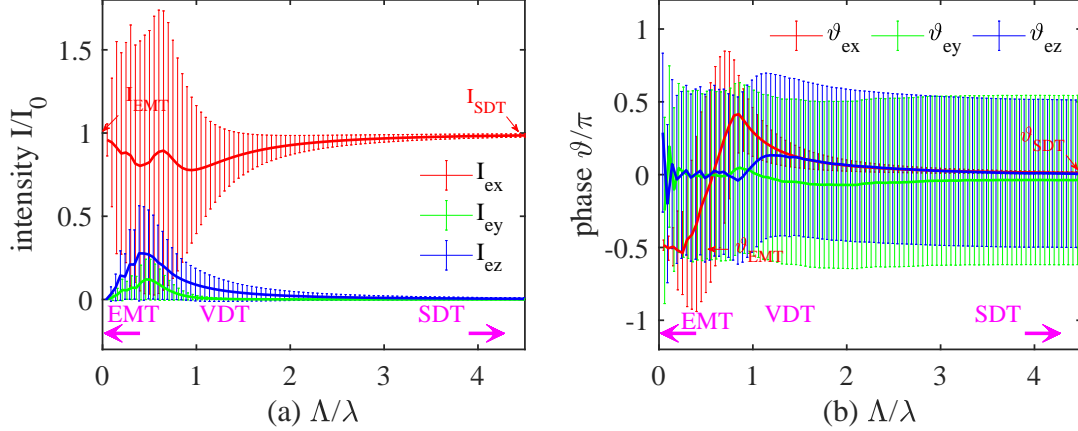


FIG. 2. Statistic analyses for (a) transmissive intensity I and (b) the field phase ϑ of the central pixel over ensembles of 3000 kinoforms versus pixel size Λ , in the case of normal illuminations.

pixels with thickness $d_{ij} = \lambda$, and are stochastically patterned with 0 ($n_0 = 1$) or 1 ($n_1 = 1.5$) components, except for the central one being 0. Numerical results for (a) the transmissive intensity of the central pixel and (b) the corresponding field phase at the exit plane are shown in Fig. 2. It is found that: (I) on condition $\Lambda/\lambda \gg 1$, the transmissive intensity and the phase converge well to the values $I_{\text{SDT}} = I_0$ and $\vartheta_{\text{SDT}} = 0$ by scalar model; (II) on condition $\Lambda/\lambda \ll 1$, numerical results fit in with the values $I_{\text{EMT}} = 0.95I_0$ and $\vartheta_{\text{EMT}} = -0.5\pi$ by the effective medium theory (EMT)¹⁶ (effective refractive index $n_{\text{EMT}} = 1.25$); (III) on condition $\Lambda/\lambda \approx 1$, the transmissive intensity and the phase with respect to different polarizations present significant deviations from SDT, stating a demand for the vector diffraction theory (VDT). Ruan’s paper¹⁶ analyzes a specified blazed grating and points out similar findings: SDT is valid for $\Lambda/\lambda \geq 5$ at normal incidence and for $\Lambda/\lambda \geq 10$ at oblique incidence; EMT is valid when higher-order diffractions appear in the form of evanescent waves, i.e. $\Lambda/\lambda \ll 1$.

For these reasons, this paper presents an efficient vector diffraction theory to treat the issue over the deviation of SDT calculations at $\Lambda/\lambda \leq 1$ condition. By the tight-binding presumption, the transfer matrix \mathbf{T}_{ij} in Fig. 1 is considered to be strongly dependent on the structure ϕ_{ij} of the local pixel that the matrix stands for, and that of other finite nearest-neighboring (NN) ones, called OTB. For instance, the 3x3-NN OTB approximation means that the transmissive field of a pixel, except itself, only interacts with the fields of the surrounding 8 pixels (within a 3x3 block). Its matrix form of the transfer matrix is expressed

$$\begin{aligned}
\mathbf{T}_{ij} &= \mathbf{\Omega} \mathbf{\Phi}_{ij,NN} \\
&= \begin{bmatrix} \boxed{C_{e_{x,i} \rightarrow e_{x,o}}} & \boxed{C_{e_{y,i} \rightarrow e_{x,o}}} & \boxed{C_{e_{z,i} \rightarrow e_{x,o}}} \\ \boxed{C_{e_{x,i} \rightarrow e_{y,o}}} & \boxed{C_{e_{y,i} \rightarrow e_{y,o}}} & \boxed{C_{e_{z,i} \rightarrow e_{y,o}}} \\ \boxed{C_{e_{x,i} \rightarrow e_{z,o}}} & \boxed{C_{e_{y,i} \rightarrow e_{z,o}}} & \boxed{C_{e_{z,i} \rightarrow e_{z,o}}} \end{bmatrix} \begin{bmatrix} \boxed{P_{e_x}} & \boxed{0} & \boxed{0} \\ \boxed{0} & \boxed{P_{e_y}} & \boxed{0} \\ \boxed{0} & \boxed{0} & \boxed{P_{e_z}} \end{bmatrix}
\end{aligned}$$

FIG. 3. The transfer matrix of the OTB model in matrix form.

in Fig. 3, where $\mathbf{\Omega}$ is a constant 3×3 M-matrix that can be pre-determined with given optical set-ups by fitting rigorous electromagnetic simulations. $\mathbf{\Phi}_{ij,NN}$ is $3M \times 3$ matrix, which labels whether the local pixel ij and other finite NN ones occupy (label 1) or non-occupy (label 0) the corresponding basis state (see Fig. 4). The diagonal block responds to different field polarizations. Here M defines the number of basis states under a specified scheme. This work applies a simple scheme: for a u -level CGH under vxv-NN OTB approximation, a w -pixel-grouping scheme gives $M = u^w (v^2 - 1)(w - 1)^{-1}$. The term u^w stands for $u \times u \times u \dots$ kinds of pixel profiles for w pixels in a group. The remaining term represents how number groups can be categorized, where the central one is the subjective group member due to the tight-binding presumption. The definition of the transfer matrix in Fig. 3 presents a clear physical interpretation: the matrix $\mathbf{\Phi}$ is the occupying probability of basis states, while the matrix $\mathbf{\Omega}$ accounts for how the fields transmit through those states. Figure 4 quantitatively demonstrates the OTB basis states for 2-level CGHs under 2x2-NN scenario, where the basis components are categorized according to the 2-pixel-grouping (2-p.-g.) and 4-pixel-grouping (4-p.-g.) schemes. The corresponding vectors $p_{e_{\{x,y,z\}}}$ (components of $\mathbf{\Phi}$), which label the population state of the exemplary 2x2-pixel block at upper-left corner, are also depicted, respectively.

For numerical analyses, Figs. 5-6 illustrate two sets of CGHs which are generated by SDT and OTB. Additional rigorous electromagnetic computations by FDTD¹⁹ for these generated CGHs are also applied to represent their accurate optics. In Fig. 5, we design four 4-level CGHs for letter-A target intensity by SDT, 2-pixel-grouping OTB ($M = 128$), 5-pixel-grouping OTB ($M = 2048$), and 9-pixel-grouping OTB models ($M = 4^9$), respectively.

OTB bases for 2-level CGHs under 2x2-NN scenario

I	II	basis of 2-p.-g. (M=12)	$\begin{bmatrix} 00\rangle_{I,II} \\ 01\rangle_{I,II} \\ 10\rangle_{I,II} \\ 11\rangle_{I,II} \\ 00\rangle_{I,III} \\ 01\rangle_{I,III} \\ 10\rangle_{I,III} \\ 11\rangle_{I,III} \\ 00\rangle_{I,IV} \\ 01\rangle_{I,IV} \\ 10\rangle_{I,IV} \\ 11\rangle_{I,IV} \end{bmatrix}$	basis of 4-p.-g. (M=16)	$\begin{bmatrix} 0000\rangle_{I-VI} \\ 0001\rangle_{I-VI} \\ 0010\rangle_{I-VI} \\ 0011\rangle_{I-VI} \\ 0100\rangle_{I-VI} \\ 0101\rangle_{I-VI} \\ 0110\rangle_{I-VI} \\ 0111\rangle_{I-VI} \\ 1000\rangle_{I-VI} \\ 1001\rangle_{I-VI} \\ 1010\rangle_{I-VI} \\ 1011\rangle_{I-VI} \\ 1100\rangle_{I-VI} \\ 1101\rangle_{I-VI} \\ 1110\rangle_{I-VI} \\ 1111\rangle_{I-VI} \end{bmatrix}$
III	IV				

$$\begin{aligned}
 p_{e_x,2pg} &= p_{e_y,2pg} = p_{e_z,2pg} = [100001000100]^t \\
 p_{e_x,4pg} &= p_{e_y,4pg} = p_{e_z,4pg} = [0001000000000000]^t
 \end{aligned}$$

FIG. 4. Definitions of OTB basis states for 2-level (white and gray) CGHs under 2x2-NN scenario, according to the 2-pixel-grouping (2-p.-g.) and 4-pixel-grouping (4-p.-g.) schemes. The corresponding vectors $p_{e_{\{x,y,z\}}}$, which label the population state of the exemplary 2x2-pixel block at upper-left corner, are also depicted, respectively.

The relevant parameters are: the normalized pixel size $\Lambda/\lambda = 0.7$, the quantized pixel thickness $\lambda/2$, the total pixel number 65x65, the refractive index of the materials $n = 1.5$, and the usage of 3x3-NN OTB approximation. The constant matrix $\mathbf{\Omega}$ is pre-computed by fitting optics of all possible patterns in a 3x3-pixel block using RCWA. Numerical results indicate that the CGH by SDT characterizes strong zero-order intensity in the far-field, and expresses an incorrect intensity distribution as observing its accurate optics (by FDTD). The CGHs from the OTB models, however, give more accurate optics similar to the target, although the results reveal a trade-off property between accuracy and efficiency (By comparing structures II to IV, it is found that the intensity of the far-field becomes more accurate as increasing the number of basis states in computations). In Fig. 6, we evaluate another star-wireframe example, with different parameters including the normalized grid pitch $\Lambda/\lambda = 0.4$, the quantized pixel thickness λ , the pixel number 121x121, and the usage of 5x5-NN OTB approximation. The result shows that the higher-order OTB can function correctly for CHGs having pixels at a lower scale.

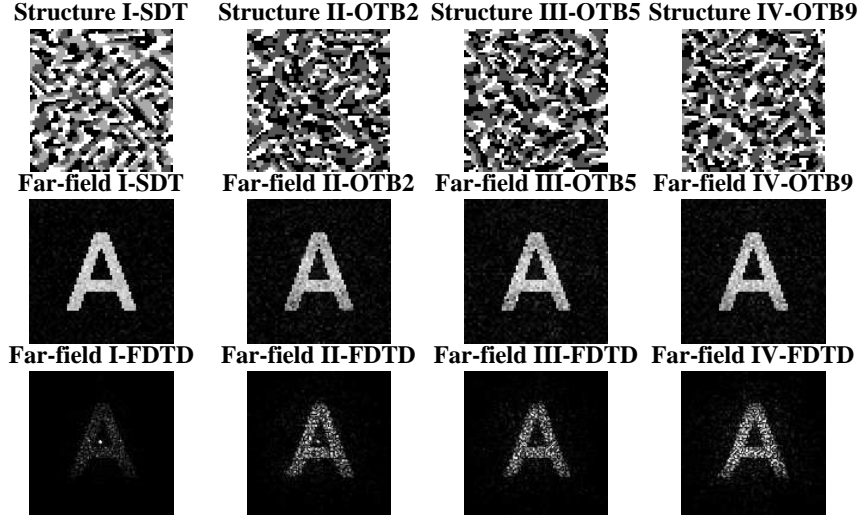


FIG. 5. Comparisons of 4-level CGH structures and the reconstructed far-field intensities for English letter A by SDT, OTB₂, OTB₅, and OTB₉, respectively. Accurate far-field intensities corresponding to structures I – IV by the FDTD method are depicted in the last row of the diagram. Relevant parameters are $\Lambda/\lambda = 0.7$ and 3x3-NN for OTB.

This paper presents an efficient optical tight-binding model in vector representation, so as to design macroscopic (mm- to cm-scale diameter) CGHs with subwavelength feature size. A simple Matlab code can be downloaded online²⁰, in which the complete bases (by 9-pixel-grouping scheme) on the 3x3-NN OTB approximation are used so that components of transfer matrices can be determined directly by RCWA. Implemented with standard CPU-GPU hybrid computers, it is estimated to that the OTB-process can complete simulated-annealing optimizations on thin CGHs having 2048x2048 pixels in 24 hours. In the future, we expect to explore applications associated with liquid crystal materials (anisotropic RCWA¹⁸), and survey new optic devices having hybrid pixel scales ($\Lambda/\lambda \geq 1$ and $\Lambda/\lambda \ll 1$ at the same time).

I. ACKNOWLEDGEMENT

This work was supported by ChiMei Visual Technology Corporation under Project no. 37.

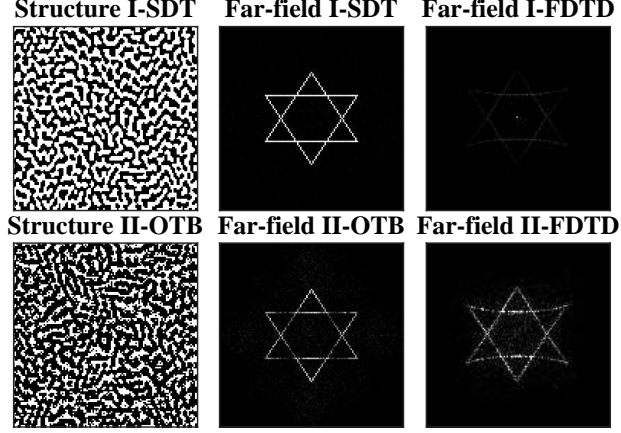


FIG. 6. Comparisons of 2-level CGH structures and the reconstructed far-field intensities for a star wireframe by SDT and OTB₂₅, respectively. Accurate far-field intensities corresponding to structures I – II by the FDTD method are depicted in the last column of the diagram. Relevant parameters are $\Lambda/\lambda = 0.4$ and 5x5-NN for OTB.

REFERENCES

- ¹A. Forbes, A. Dudley, and M. McLaren, "Creation and detection of optical modes with spatial light modulators", *Adv. Opt. Photonics* 8, 200 (2016).
- ²C. Rosales-Guzman, and A. Forbes, "How to shape light with spatial light modulators", SPIE Press (2017).
- ³B. Pesach, and Z. Mor, inventor; Apple Inc, assignee, "Projectors of structured light", United States patent US US20130038881A1 (2013, Feb 14).
- ⁴K. Dholakia, M. MacDonald, and G. Spalding, "Optical tweezers: the next generation", *Phys. World* 15, 31 (2002).
- ⁵Y. V. Miklyaev, W. Imgrunt, V. S. Pavelyev, D. G. Kachalov, T. Bizjak, L. Aschke, and V. N. Lissotschenko, "Novel continuously shaped diffractive optical elements enable high efficiency beam shaping", *Proc. SPIE* 7640, Optical Microlithography XXIII, 764024 (2010).
- ⁶V. Boyer, R. M. Godun, G. Smirne, D. Cassetari, C. M. Chandrashekar, A. B. Deb, Z. J. Laczik, and C. J. Foot, "Dynamic manipulation of Bose-Einstein condensates with a spatial light modulator", *Phys. Rev. A* 73, 031402 (2006).
- ⁷C. S. Hwang, Y. H. Kim, G. H. Kim, J. H. Yang, S. Cheon, S. M. Cho, K. Choi, J. H.

- Choi, J. E. Pi, C. Y. Hwang, H. O. Kim, W. J. Lee, and H. B. Kang, "Development of spatial light modulator with ultra fine pixel pitch for electronic holography", Proc. SPIE 10666, Three-Dimensional Imaging, Visualization, and Display 2018, 1066605 (2018).
- ⁸H. Hao, Z. Tingting, S. Qiang, and Y. Xiaodong, "Wide angle 2D beam splitter design based on vector diffraction theory", Opt. Comm. 434, 28 (2019).
- ⁹N. Bhebbhe, P. A. C. Williams, C. Rosales-Guzman, V. Rodriguez-Fajardo, and A. Forbes, "A vector holographic optical trap", Sci. Rep. 8, Article number 17387 (2018).
- ¹⁰S. J. Byrnes, A. Lenef, F. Aieta, and F. Capasso¹, "Designing large, high-efficiency, high-numericalaperture, transmissive meta-lenses for visible light", Opt. Express 24(5), 5110 (2016).
- ¹¹R. Piestun and J. Shamir, "Synthesis of three-dimensional light fields and applications", Proc. IEEE 90, 222244 (2002).
- ¹²Y. W. Chen, S. Yamauchi, N. Wang, and Z. Nakao, "A fast kinoform optimization algorithm based on simulated annealing", IEICE Trans. Fundamentals E83A(4), 774 (2000).
- ¹³J. Jiang, G.P. Nordin, "A rigorous unidirectional method for designing finite aperture diffractive optical elements", Opt. Express 7, 237 (2000).
- ¹⁴M. E. Testorf, and M. A. Fiddy, "Efficient optimization of diffractive optical elements based on rigorous diffraction models", J. Opt. Soc. Amer A 18, 2908 (2001).
- ¹⁵F. Di, Y. Yingbai, J. Guofan, T. Qiaofeng, H. Liu, "Rigorous electromagnetic design of finite-aperture diffractive optical elements by use of an iterative optimization algorithm", J. Opt. Soc. Amer A 20, 1739 (2003).
- ¹⁶D. Ruan, L. Zhu, X. Jing, Y. Tian, L. Wang, and S. Jin, "Validity of scalar diffraction theory and effective medium theory for analysis of a blazed grating microstructure at oblique incidence", App. Opt. 53(11), 2357 (2014).
- ¹⁷J. Jiang, "Rigorous analysis and design of diffractive optical elements", doctoral dissertation, University of Alabama in Huntsville (2000).
- ¹⁸I. L. Ho, Y. C. Chang, C. H. Huang, and W. Y. Li, "A detailed derivation of rigorous coupled wave algorithms for three-dimensional periodic liquid-crystal microstructures", Liq. Cryst. 38(2), 241 (2011).
- ¹⁹<https://optiwave.com/resources/academia/free-fdtd-download/>
- ²⁰submitting.